Changing the Inhibitory Specificity and Function of the Proteinase Inhibitor Eglin c by Site-Directed Mutagenesis: Functional and Structural Investigation†

Dirk W. Heinz,‡,§ Sven G. Hyberts,‖ Jeff W. Peng,‖ John P. Priestle,‡ Gerhard Wagner,*,‖ and Markus G. Grütter*,‡

Pharmaceutical Research Division, Ciba-Geigy Ltd., CH-4002 Basel, Switzerland, and Department of Biological Chemistry and Molecular Biology, Harvard Medical School, Boston, Massachusetts 02115

Received February 19, 1992; Revised Manuscript Received May 28, 1992

ABSTRACT: Amino acids in the serine proteinase inhibitor eglin c important for its inhibitory specificity and activity have been investigated by site-directed mutagenesis. The specificity of eglin c could be changed from elastase to trypsin inhibition by the point mutation Leu45 → Arg (L45R) in position P1 [nomenclature according to Schechter and Berger (1967) *Biochem. Biophys. Res. Commun. 27*, 157–162]. Model building studies based on the crystal structure of mutant L45R [Heinz et al. (1991) *J. Mol. Biol. 217*, 353–371] were used to rationalize this specificity change. Surprisingly, the double mutant L45R/D46S was found to be a substrate of trypsin and various other serine proteinases. Multidimensional NMR studies show that wild-type eglin c and the double mutant have virtually identical conformations. In the double mutant L45R/D46S, however, the N–H bond vector of the scissile peptide bond shows a much higher mobility, indicating that the internal rigidity of the binding loop is significantly weakened due to the loss or destabilization of the internal hydrogen bond of the P1′ residue. Mutant T44P was constructed to examine the role of a proline in position P2, which is frequently found in serine proteinase inhibitors [Laskowski and Kato (1980) *Annu. Rev. Biochem. 49*, 593–626]. The mutant remains a potent elastase inhibitor but no longer inhibits subtilisin, which could be explained by model building. Both Arg51 and Arg53, located in the core of the molecule and participating in the hydrogen bonding network with residues in the binding loop to maintain rigidity around the scissile bond, were individually replaced with the shorter but equally charged amino acid lysine. Both mutants showed a decrease in their inhibitory potential. The crystal structure of mutant R53K revealed the loss of two hydrogen bonds between the core and the binding loop of the inhibitor, which are partially restored by a solvent molecule, leading to a decrease in inhibition of elastase by 2 orders of magnitude.

Serine proteinases are involved in nearly every aspect of life, e.g., protein digestion and regulatory mechanisms such as complement activation and blood coagulation [reviewed by Neurath (1984)]. They are also recognized as possible pathogenic factors in a number of diseases (Hörl & Heidland, 1982), which has led to intensive studies of proteinase inhibitors as potential drugs [reviewed by Schnebli and Braun (1986)]. In general, proteinaceous proteinase inhibitors act as pseudosubstrates, however with extremely slow turnover (Laskowski & Kato, 1980). The crystal structures of proteinase inhibitors in complex with their target enzymes have provided insights into the structural prerequisites necessary for specific inhibition [reviewed by Read and James (1986) and Bode and Huber (1992)]. The predominant structural feature of these inhibitors is the so-called reactive site binding loop, which is highly complementary to the active site region of the enzyme and which resembles closely the conformation of a peptide substrate when bound to the enzyme. In contrast to a flexible peptide substrate, the binding loop is held in a rigid conformation which prevents it from being cleaved at the "scissile bond". This rigidity is maintained by covalent (i.e., disulfide bridges) or noncovalent interactions between residues located in the binding loop and the rest of the molecule.

The amino acid located in position P1 (Schechter & Berger, 1967) is chiefly responsible for the inhibitory specificity of serine proteinase inhibitors (Laskowski & Kato, 1980; Laskowski et al., 1981). A mutation at this position should therefore have a large effect on the inhibitory specificity. A number of specificity changes caused by mutations of amino acids located in position P1 of different serine proteinase inhibitors have been reported (e.g., Leary & Laskowski, 1973; Wenzel et al., 1976; Owen et al., 1983; Jallat et al., 1986; McWerther et al., 1989; Longstaff et al., 1990; Komiyama et al., 1991; Kojima et al., 1991; Sinha et al., 1991).

To further investigate the structural basis of binding loop stabilization and inhibitory specificity in proteinaceous proteinase inhibitors, amino acid substitutions were performed in the inhibitor eglin c, a 70 amino acid containing protein isolated from the leech *Hirudo medicinalis* (Seemüller et al., 1977). Eglin c belongs to the potato I inhibitor family (Laskowski et al., 1981) and strongly inhibits human leukocyte elastase (HLE), cathepsin G, α-chymotrypsin, and subtilisin, but not trypsin (Seemüller et al., 1980). The gene encoding the protein has been synthesized and expressed in *Escherichia coli* (Rink et al., 1984), yielding a convenient source of recombinant eglin c (referred to in the following simply as eglin). The crystal structure of eglin in complex with subtilisin Carlsberg (McPhalen et al., 1985; Bode et al., 1986a) consists of a small globular core and an exposed active site binding loop (Figure 1). The binding loop which harbors the scissile peptide bond between Leu45 (P1) and Asp46 (P1′) is held in a rigid conformation by hydrogen bond interactions between three residues located in the binding loop (Thr44, Asp46, and Arg48), three residues located in the core (Arg51,

† This work was supported by the National Institute of Health (Grant GM38608).

* Authors to whom correspondence should be addressed.

‡ Ciba-Geigy Ltd.

§ Present address: Institute of Molecular Biology and Howard Hughes Medical Institute, University of Oregon, Eugene, OR 97403.

‖ Harvard Medical School.

[1] Abbreviations: HLE, human leucocyte elastase; BPTI, bovine pancreatic trypsin inhibitor: NMR, nuclear magnetic resonance spectroscopy; 2D, two-dimensional; 3D, three-dimensional. Work described in this paper is part of the Ph.D. Thesis of D.W.H. (Heinz, 1990).

0006-2960/92/0431-8755$03.00/0

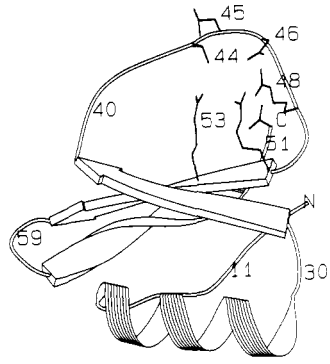

FIGURE 1: RIBBON diagram (Priestle, 1988) illustrating the secondary structure of eglin. The following residues are involved in the stabilization of the binding loop: Arg51, Arg53, Arg48, Thr44, Asp46, and the carboxy terminus. The P1 residue, Leu45, is also indicated. The scissile bond is located between residues Leu45 and Asp46.

Arg53, and the C-terminal Gly70), and a number of internally bound solvent molecules. In addition, an intraresidual hydrogen bond which is formed between the side chain of Asp46 and its own amide proton is assumed to be critical for binding loop stabilization (Bode et al., 1986a; Wagner et al., 1990).

In this paper, we describe the construction and the functional and structural characterization of five eglin mutants containing point mutations in the binding loop and in positions in the core which are believed to be involved in the stabilization of the binding loop. Functional properties were evaluated by steady-state inhibition kinetics, and structural data were obtained by X-ray crystallography, NMR spectroscopy, and model building based on the crystal structures of inhibitors and serine proteinases.

MATERIALS AND METHODS

Design of Eglin Mutants. The locations of the mutations in the sequence of eglin are shown in Table I. Mutants Leu45 → Arg (L45R), L45R/D46S, and T44P were designed on the basis of sequence comparisons with other serine proteinase inhibitors. Mutant L45R was constructed to test whether eglin could be changed to an inhibitor of trypsin or thrombin which prefer basic amino acids in position P1. Most of the trypsin and thrombin inhibitors belonging to the Bowman-Birk inhibitor, potato inhibitor II, and α1-proteinase related inhibitor families contain a well-conserved serine in position P1′ following an arginine or lysine in position P1 (Laskowski & Kato, 1980). The double mutant L45R/D46S was constructed to test whether these mutations could change eglin to a thrombin inhibitor on the basis of the sequence comparisons described above. Mutant T44P was constructed to improve the binding of eglin to HLE which seems to interact favorably with substrates or inhibitors containing a proline in position P2 (Bode et al., 1989a) and based on the fact that many natural HLE inhibitors contain a well-conserved proline at this position (Laskowski et al., 1987). Both mutants T44P and L45R/D46S were also made to examine the role of Thr44 and Asp46 in maintaining the implied vital rigidity of the binding loop by interacting with residues located in the core of eglin. The conservative point mutations R51K and R53K in the core of eglin were constructed to investigate the relative contribution of both arginines to the noncovalent stabilization of the binding loop.

Site-Directed Mutagenesis and Purification. Plasmid pML147 used for the expression of recombinant eglin (Rink et al., 1984) was obtained from Dr. M. Liersch (Ciba-Geigy Ltd., Basel). Site-directed mutagenesis of eglin was performed in M13mp8 (Messing, 1983) according to the primer extension method of Zoller and Smith (1983). Mutagenic oligonucleotides (18–22 bases in length) were synthesized and purified by H. Rink (Ciba-Geigy Ltd., Basel). *E. coli* strain BMH71-18mutS (Kramer et al., 1984) was transformed with mutagenized phage M13mp8. Phages containing mutant eglins were screened by colony hybridization (Grunstein & Hogness, 1975) using ^{32}P-phosphorylated mutagenic primers. Mutants were confirmed by dideoxy sequencing (Sanger et al., 1977). Eglin mutants were expressed in *E. coli* JA221 (Clarke & Carbon, 1978) under the control of the tryptophan promoter (Rink et al., 1984).

E. coli cells producing mutant eglins were grown by fermentation as described (Rink et al., 1984). After centrifugation, cells were suspended in 20 mM Tris-HCl buffer, pH 7.8, and disrupted using a dyno mill. Cell debris was removed by centrifugation. The high resistance of eglin to denaturation by acid (Seemüller et al., 1977) was used to precipitate most contaminant proteins by adding acetic acid to a final concentration of 2%. Viscosity of the solution was reduced by adding DNase I (10 mg/L). Precipitate was removed by centrifugation, and the supernatant was lyophilized (Virtis, Gardiner, NY). The dry lyophilisate was dissolved in a small volume of 20 mM ammonium carbonate buffer, pH 7.5, and applied to a gel filtration column (Sephadex G50SF, Pharmacia, Uppsala, Sweden). Eglin mutants were eluted in ammonium carbonate buffer and subsequently lyophilized leading to approximately 100–200 mg of pure protein/L of fermenter solution.

Protein Chemical Characterization. Eglin mutants were shown to be homogeneous by SDS–PAGE on silver-stained gels containing 20% polyacrylamide (Laemmli, 1970) and reversed-phase HPLC (Millipore–Waters, Milford, MA). The isoelectric points (p*I*) of the mutants were determined by isoelectric focusing using Ampholine PAG plates (LKB-Pharmacia, Uppsala, Sweden) in the pH range of 3.5–9.5 and using a p*I* calibration kit containing reference proteins with p*I* values ranging from 3 to 10. The p*I* value of wild-type eglin is 5.4. Only mutants L45R (p*I* = 6.1) and L45R/D46S (p*I* = 6.7) deviated from this value due to the additional positive charge and the loss of a negative charge, respectively. The mass of eglin mutants was determined by mass spectrometry, performed by F. Raschdorf (Ciba-Geigy Ltd., Basel) using the fast atom bombardment method. MH^+ peaks with an accuracy of ±1 Da could be obtained (Barber et al., 1984). Mutants were compared with wild-type eglin using CD spectroscopy (in the laboratory of Dr. P. Moser, Ciba-Geigy Ltd., Basel) to confirm that they were correctly folded. Measurements were performed on a Jasco J-20 spectropolarimeter at 25 °C and 90 °C. No significant differences in their secondary structures were detected on comparison with the wild-type spectrum.

Kinetic Measurements. Active-site-titrated HLE was obtained from Dr. H.-P. Schnebli (Ciba-Geigy Ltd., Basel). 1-(Tosylamino)-2-phenylethyl chloromethyl ketone- (TPCK-) treated bovine pancreatic trypsin was from Worthington (Freehold, NJ). It was active-site-titrated using *p*-nitrophenyl *p*-guanidinobenzoate hydrochloride (Fluka, Switzerland) as described (Chase & Shaw, 1970). Subtilisin (from *Bacillus subtilis*) was from Boehringer (Mannheim, Germany) and was active-site-titrated using analytically pure wild-type eglin, which has previously been equivalence titrated with HLE as described (Braun et al., 1987). Human thrombin was from Sigma (St. Louis, MO). The following peptide substrates were used for kinetic experiments: MeO-Suc-Ala-Ala-Pro-

Table I: Locations of Mutations in the Eglin Sequence[a]

	Mutations in the Binding Loop of Eglin								
position	41	42	43 P3	44 P2	45 P1	46 P1′	47 P2′	48 P3′	49
wild-type eglin	-Ser-	Pro-	Val-	Thr-	Leu-	Asp-	Leu-	Arg-	Tyr-
mutant L45R	-Ser-	Pro-	Val-	Thr-	Arg-	Asp-	Leu-	Arg-	Tyr-
mutant L45R/D46S	-Ser-	Pro-	Val-	Thr-	Arg-	Ser	Leu-	Arg-	Tyr-
mutant T44P	-Ser-	Pro-	Val-	Pro-	Leu-	Asp	Leu-	Arg-	Tyr-

	Mutations in the Core of Eglin						
position	49	50	51	52	53	54	55
wild-type eglin	-Tyr	-Asn	-Arg	-Val	-Arg	-Val	-Phe-
mutant R51K	-Tyr	-Asn	-Lys	-Val	-Arg	-Val	-Phe-
mutant R53K	-Tyr	-Asn	-Arg	-Val	-Lys	-Val	-Phe-

[a] The scissile peptide bond is located between residues 45 and 46.

Val-*p*-nitroanilide (pNA) (specific for HLE: K_M = 2.0 × 10^{-4} M) and Bz-L-Arg-pNA (specific for trypsin: K_M = 3.8 × 10^{-4} M) were from Bachem (Bubendorf, Switzerland); MeO-Suc-Arg-Pro-Tyr-pNA (specific for subtilisin: K_M = 0.8 × 10^{-4} M) and D-Phe-Pip-Arg-pNA (specific for thrombin) were from KabiVitrum (Stockholm, Sweden). Michaelis constants K_M listed above were determined as described by Michal (1984). The following buffers and solutions were used for the inhibition assays: PBS Dulbecco (Oxoid, Basingstoke, England), 0.15 μM human serum albumin for HLE; 0.2 M triethanolamine, 20 mM $CaCl_2$, pH 7.8 for trypsin; 50 mM Tris-HCl, 100 mM $CaCl_2$, pH 8.5, for subtilisin; 50 mM Tris-HCl, 100 mM NaCl, 0.1% PEG 6000, pH 8, for thrombin. Equivalence titrations were performed as described (Braun et al., 1987). Throughout all kinetic experiments, the concentrations of HLE, trypsin, and subtilisin and their inhibitors are given in molarities of "active" molecules.

Equilibrium dissociation constants, K_i, describing the interactions of eglin mutants with the selected serine proteinases elastase, trypsin, and subtilisin were determined according to Bieth (1974) and Braun et al. (1987) in the laboratory of Dr. H.-P. Schnebli (Ciba-Geigy Ltd., Basel) using a recording Uvikon 820 spectrophotometer (Kontron, Switzerland) equipped with a constant temperature sample holder and modified to allow the use of a magnetic stirrer in the cuvette. K_i was determined by measuring the enzymatic activity of mixtures containing constant amount of substrates (4–20 times K_M) preincubated with increasing amounts of inhibitor. After addition of the enzyme, the release of *p*-nitroaniline was recorded until steady-state reaction rates could be measured, i.e., until the curve (OD_{405} vs time) was linear for at least 20 min. $K_{i(app)}$ and K_i were calculated for each inhibitor concentration from the following relationship and averaged (Braun et al., 1987):

$$K_{i(app)} = K_i(1 + [S_0]/K_M) = \frac{V_i/V_0}{(1 - V_i/V_0)}[I_0] - V_i/V_0[E_0]$$

where V_0 and V_i are the steady-state rates for free enzyme and enzyme in presence of inhibitor, respectively, and $[S_0]$, $[E_0]$, and $[I_0]$ are the total concentrations of substrate, enzyme, and inhibitor in the cuvette. A family of inhibition curves is shown in Figure 2 for the inhibition of HLE by mutant R51K.

Preliminary inhibition experiments with thrombin were undertaken with wild-type eglin and the mutants L45R and L45R/D46S. Control measurements were performed with hirudin, a potent natural thrombin inhibitor (K_i = 10^{-14} M; Stone & Hofsteenge, 1986). A total of 500 pmol of thrombin was mixed with the eglin molecule (in 10-fold excess) and incubated at 37 °C for 10 min. After addition of 2 mM

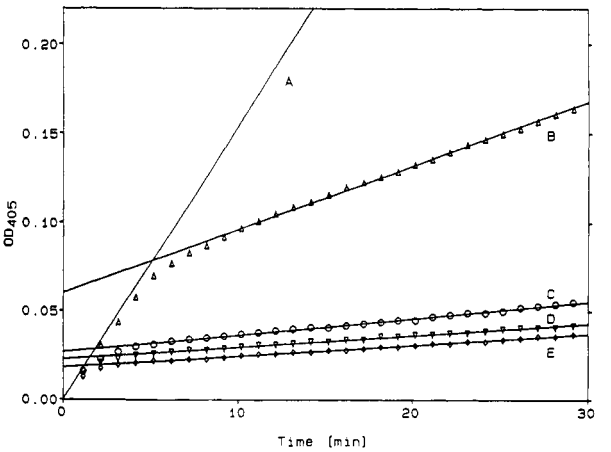

FIGURE 2: Hydrolysis of 0.89 mM substrate (MeO-Suc-A-A-P-V-pNA) by 8.4 nM HLE in the absence of mutant R51K (curve A) and in the presence of 8.4 nM (curve B), 16.8 nM (curve C), 25.2 nM (curve D), and 33.6 nM (curve E) mutant R51K. The slopes of the steady-state parts of the curves (calculated by linear regression) represent V_0 (absence of inhibitor) and V_i (presence of inhibitor) (see text).

substrate, the increase in optical density at 405 nm was measured and compared with substrate consumption by thrombin alone.

Timed proteinase–inhibitor incubation mixtures were analyzed by gel electrophoresis to discriminate whether mutant eglins are in fact inhibitors or substrates or whether they bound to the enzyme at all. Mutant eglins (in a final concentration of 200 μM) were incubated in a molar excess with their putative target enzyme. Samples were taken at predetermined times and analyzed immediately by SDS gel electrophoresis. A decay or absence of the band representing the eglin mutant indicated the mutant being a substrate of the respective enzyme. Additional bands of lower molecular weight indicated the cleavage of the eglin molecules upon binding to the enzyme.

Crystal Structure Analysis and Model Building Studies. The crystal structures of complexes formed between subtilisin Novo and the eglin mutants L45R (to 2.1-Å resolution) and R53K (to 2.4-Å resolution) were solved by molecular replacement and difference Fourier techniques, respectively. Details about crystallization, structure determination and interpretation are described by Heinz et al. (1991). Mutant L45R could be co-crystallized with bovine trypsin. Unfortunately, the crystals were not suitable for structure solution.

Model building studies were performed using an interactive Evans & Sutherland PS390 graphics display system and a modified version (Rice version 6.6; Pflugrath et al., 1984) of the program FRODO (Jones, 1978). The model complex of

mutant L45R with trypsin was built on the basis of the structural similarity of eglin and bovine pancreatic trypsin inhibitor (BPTI) in their binding loops and the crystal structures of mutant L45R and the BPTI–trypsin complex (Huber et al., 1974). Details of the superposition are described by Heinz et al. (1991). A model of the complex between wild-type eglin and HLE was kindly provided by Dr. W. Bode (Max-Planck-Institut, Martinsried, Germany). It has been constructed on the basis of the structures of wild-type eglin and the complex formed between HLE and the third domain of the ovomucoid inhibitor (Bode et al., 1986b). The point mutations in the models of mutants T44P and R51K were introduced into the wild-type structure using optimized stereochemistry for the changed residues.

NMR Spectroscopy. The assignments of the NMR resonances of eglin c and the double mutant were performed using standard assignment techniques (Wagner & Wüthrich, 1982). The assignments of the wild-type protein were described previously (Hyberts & Wagner, 1989). NOESY spectra of wild-type and mutant protein were recorded using standard methods (Jeener et al., 1979; Anil Kumar et al., 1980; Macura et al., 1981). All spectra were recorded at 30 °C, pH 3.0. Two-dimensional heteronuclear proton detected ^{15}N–^{1}H correlated spectra were recorded with an antiphase evolution period as described originally by Vindusek et al. (1982). ^{15}N relaxation times and heteronuclear NOEs were measured with techniques described by Peng et al. (1991) and Peng and Wagner (1992). ^{15}N-Labeled wild-type eglin and mutant L45R/D46S were produced by growing cells in minimal media containing ^{15}N-labeled NH_4Cl (99% enriched; Cambridge Isotope Laboratories, Innerberg, Switzerland) as the sole nitrogen source. The completeness of ^{15}N-labeling was confirmed by mass spectrometry. For the measurements of the temperature coefficients of amide resonances, heteronuclear ^{15}N–^{1}H correlated spectra were recorded at different temperatures. The chemical shifts were referenced relative to 3-(trimethylsilyl) [2,2,3,3-$^{2}H_4$]propionate (TSP). The pH dependence of the NH resonances was studied using 2D heteronuclear ^{15}N–^{1}H correlated spectra, recorded at 36 °C. Heteronuclear ^{15}N–^{1}H vicinal coupling constants were measured in ^{15}N-enriched samples using the technique analogous to those described by Montelione et al. (1989). In particular, 2D TOCSY spectra (Braunschweiler & Ernst, 1983) of uniformly ^{15}N-enriched eglin c and the double mutant were recorded using a DIPSI-2 spin lock (Shaka et al., 1988). To solve problems of resonance overlap, two 3D NOESY spectra (Wider et al., 1989) of these two samples were recorded with the following pulse sequence:

$$90°(^{1}H)\text{–}\tau\text{–}90°(^{15}N)\text{–}t_{1/2}\text{–}180°(^{1}H)\text{–}t_{1/2}\text{–}90°(^{15}N)\text{–}\tau\text{–}t_2\text{–}90°(^{1}H)\text{–}\tau_m\text{–}90°(^{1}H)\text{–acq}$$

RESULTS

Inhibitory Activity of Eglin Mutants. Equilibrium dissociation constants, K_i, describing the interactions of mutant eglins and the serine proteinases HLE, trypsin, and subtilisin are listed in Table II. None of the eglin mutants reaches the strong inhibitory potential of wild-type eglin against HLE (K_i = 2.0 × 10^{-11} M). Mutants T44P, R51K, and R53K are 10–100-fold weaker inhibitors, and mutant L45R shows even weaker inhibition, whereas the double mutant L45R/D46S is a substrate of HLE.

Mutant L45R strongly inhibits trypsin (K_i = 2.5 × 10^{-11} M), in contrast to wild-type eglin, which shows only weak trypsin inhibition $K_i > 10^{-5}$ M, verifying the desired specificity change from HLE to trypsin inhibition caused by the single point mutation Leu45 → Arg. Similar to the inhibition of HLE by wild-type eglin, the mechanism of trypsin inhibition by mutant L45R is fully competitive, as shown by an increase of the K_i after the substrate concentration is raised in the assay.

Table II: Equilibrium Dissociation Constants, K_i, of Eglin Mutants

a. HLE Inhibition

eglin mutant	K_i (M)
wild-type eglin	(2.0 ± 1.8) × 10^{-11}
T44P	(2.7 ± 3.2) × 10^{-10}
L45R	weak inhibitor
L45R/D46S	substrate
R51K	(6.9 ± 2.4) × 10^{-9}
R53K	(1.1 ± 1.7) × 10^{-9}

b. Trypsin Inhibition

eglin mutant	K_i (M)
wild-type eglin	weak inhibitor
L45R	(2.5 ± 2.1) × 10^{-11}
L45R/D46S	substrate

c. Subtilisin Inhibition

eglin mutant	K_i (M)
wild-type eglin	(3.2 ± 2.5) × 10^{-11}
T44P	substrate
L45R	(5.4 ± 4.0) × 10^{-11}
L45R/D46S	substrate
R51K	substrate
R53K	(1.1 ± 4.1) × 10^{-10}

In strong contrast to mutant L45R, mutant L45R/D46S is a substrate of trypsin. Besides wild-type eglin, only the mutants L45R and R53K inhibit subtilisin; mutants T44P, L45R/D46S, and R51K are substrates of this enzyme. Similar to wild-type eglin, mutants L45R and L45R/D46S, which is homologous to natural thrombin inhibitors in positions P1 and P1′, showed no inhibition of thrombin.

Mutants which did not inhibit the activity of serine proteinases in the kinetic experiments were found to be substrates of these enzymes by electrophoretic and reversed-phase HPLC analysis of timed incubation mixtures of mutant eglins and enzymes. A SDS–PAGE gel of 24-h incubation mixtures of wild-type as well as mutant eglins with HLE is shown in Figure 3a. The gel shows bands (M_r = ca. 8200) corresponding to intact wild-type eglin and the mutants R51K, L45R/D46S, R53K, L45R, and T44P. In the case of mutant L45R/D46S, the missing band demonstrates the complete proteolytic digestion of this mutant by HLE. For wild-type eglin and mutant R51K, an additional band of lower molecular weight (ca. 2500–4000) is found, representing an average of the truncated N-terminal (starting with Lys8; 38 amino acids) and C-terminal (25 amino acids) halves of the molecules caused by incomplete cleavage between residues 45 and 46 of the inhibitors during binding to HLE. In contrast, the bands of T44P and R53K remained intact. The intensity of the band of mutant L45R is reduced with no additional band of lower molecular weight.

The SDS–PAGE gel of eglin mutants alone and of 15-h incubation mixtures with bovine trypsin is shown in Figure 3b. The band of mutant L45R is unchanged, indicating complete inhibition of trypsin. The cleavage of the inhibitor upon binding to trypsin cannot be excluded. Upon incubation with trypsin (in a molar ratio of 1:1) over 24 h, a weak band of lower molecular weight representing cleaved halves of the inhibitor is visible, however, only under denaturing conditions. The band of mutant R51K and L45R/D46S completely

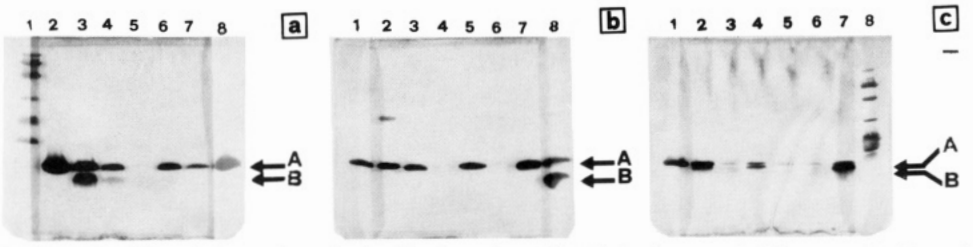

FIGURE 3: (a) SDS–polyacrylamide gel electrophoresis of eglin alone (lane 2) and of mixtures of wild-type eglin (lane 3) and eglin mutants R51K (lane 4), L45R/D46S (lane 5), R53K (lane 6), L45R (lane 7), and T44P (lane 8) (200 μM) with HLE (4 μM) after 24 h of incubation time. The band representing HLE is not visible. Bands with molecular weight labeled with A represent intact eglin, those labeled with B represent cleaved fragments of eglin (see text). The molecular weight standard proteins range from 14 000 to 82 000 (lane 1). (b) SDS–polyacrylamide gel electrophoresis of eglin mutants L45R (lane 1), R51K (lane 3), L45R/D46S (lane 5), and R53K (lane 7) and of the same mutants (200 μM) after a 15-h incubation with bovine trypsin (4 μM) (lanes 2, 4, 6, and 8). Bands of intact inhibitors are indicated by an A; those of cleaved inhibitors are indicated by a B (see text and panel a). (c) SDS–polyacrylamide gel electrophoresis of mixtures of wild-type eglin (lane 1, eglin alone; lane 2, eglin incubated) and eglin mutants T44P (lane 3), L45R (lane 4), R51K (lane 5), L45R/D46S (lane 6), and R53K (lane 7) (200 μM) with subtilisin (80 μM) after a 1-h incubation. The molecular weight standard proteins range from 14 000 to 82 000 (lane 8). The band representing subtilisin is not visible. Bands labeled with A represent intact eglin, those labeled with B represent cleaved fragments of eglin (see text and panel a).

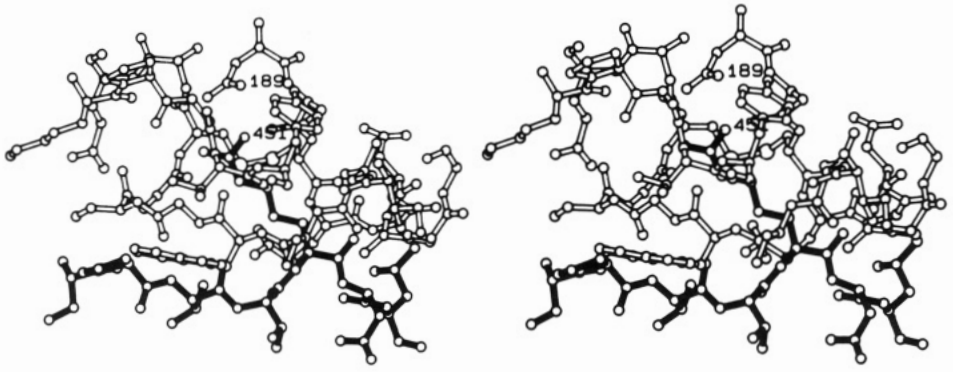

FIGURE 4: Model complex of eglin mutant L45R (solid bonds) and bovine trypsin (open bonds). Arg45 (P1) of the inhibitor fits into the S1 binding pocket of trypsin, forming a salt bridge with Asp189 at the bottom of the pocket. Residues 42–44 in the binding loop of eglin form a short antiparallel β-sheet with the enzyme.

disappeared whereas for mutant R53K a band for cleaved inhibitor appears showing that these mutants are also substrates of trypsin.

The SDS–PAGE gel of wild-type eglin alone and of a 1-h incubation of wild-type and mutant eglins with subtilisin (Figure 3c) shows intact bands for wild-type eglin and mutants L45R and R53K and the almost complete disappearance of bands corresponding to the mutants T44P, R51K, and L45R/D46S. Additional bands of lower molecular weight in the case of wild-type eglin and mutants L45R and R53K indicate a cleavage of the inhibitors during binding to subtilisin. The results obtained from the time incubations corroborate the kinetic data shown in Table II and confirm that mutants which show no interaction with their target enzymes during kinetic measurements are in fact substrates of these enzymes.

Crystal Structures and Model Building Studies. The crystal structures of mutants L45R and R53K in complex with subtilisin Novo were solved and refined at 2.1 Å and 2.4 Å, respectively (Heinz et al., 1991). To rationalize the specificity change of eglin caused by the single mutation Leu45 → Arg in position P1, the structure of mutant L45R was compared with BPTI and their binding loops comprising positions P3 to P3′ were superimposed. Despite their completely different three-dimensional folds, an excellent fit of their binding loops was found (rms deviation of main chain atoms = 0.48 Å for residues in positions P3 to P3′; Heinz et al., 1991). The model structure of the complex between mutant L45R and trypsin shows Arg45 bound into the active site cleft of trypsin and interacting with Asp189 at the bottom of the cleft. Only two "bad" contacts between both molecules are observed in the model (Figure 4).

The model structure of HLE in complex with mutant L45R shows essentially no space in the small hydrophobic active site pocket of HLE for the extended side chain of Arg45 in position P1 (figure not shown). Due to the truncation of the side chain of Arg53, Lys53 can no longer interact directly via hydrogen bonds with Thr44 located in position P2 in the binding loop of mutant R53K. Instead, atom ζ of Lys53 forms a single hydrogen bond to a solvent molecule which is itself hydrogen bonded to the main chain carbonyl oxygen of Thr44 (Heinz et al., 1991). In the model structure of mutant R51K, the side chain of Lys51 is no longer able to interact via hydrogen bonds to Asp46 in the P1′ position of the binding loop, which might increase the binding loop flexibility in the vicinity of the scissile bond (Figure 5). The model complexes of mutant T44P with subtilisin and HLE shows an excellent fit of Pro44 into the hydrophobic S2 pocket of HLE (lined by residues His57, Leu99 and Phe215) (Figure 6).

NMR Comparison of Wild Type and Mutant L45R/D46S. The mutations described here affect mainly the proteinase binding loop, and the NMR analysis was directed toward this protein region. We concentrated on the comparison between the wild-type protein and the mutant L45R/D46S since this mutant was not accessible to X-ray structure analysis. It could not be crystallized in the free form and could not be crystallized in the complex with a proteinase because it is cleaved immediately by the enzyme. To characterize the difference between the wild-type and mutant protein, we have compared the chemical shifts, the complete set of nuclear Overhauser enhancement cross-peaks in 2D NMR spectra, and homonuclear and heteronuclear vicinal coupling constants. Since hydrogen bonds are a crucial structural feature of the

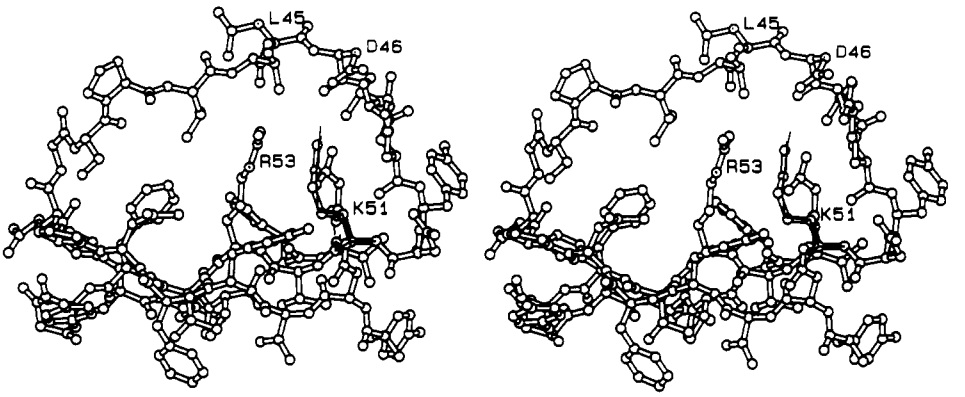

FIGURE 5: Model structure of eglin mutant R51K. The structure of the complex of wild-type eglin with subtilisin Novo (Heinz et al., 1991) was used, and the side chain of Arg51 (shown with thin bonds) was replaced with a lysine. The side chain of Lys51 is too short to interact directly with Asp46 of the binding loop in this model.

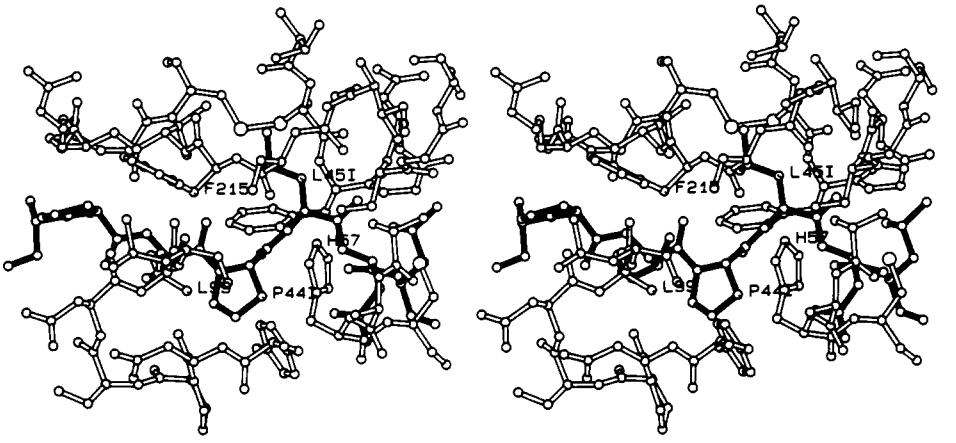

FIGURE 6: Model of eglin mutant T44P (solid bonds) with HLE (open bonds). The ϕ,ψ conformation angles of the P2 residue, Thr44, in the wild-type eglin structure are such that no alteration is necessary for the incorporation of the more restricted proline residue.

conformation of the binding loop, we also have made efforts to characterize this aspect by measuring the pH dependence and the temperature coefficients of the NH resonances. Finally, ^{15}N relaxation time measurements were performed to characterize the mobility of the polypeptide backbone.

^1H NMR Assignments and Comparison of Chemical Shifts in Wild Type and Mutant L45R/D46S. Assignment of the ^1H NMR resonances of wild-type eglin c have been described previously (Hyberts & Wagner, 1989). The assignments of the ^1H NMR resonances of mutant L45R/D46S were achieved in a similar manner. Table II shows a list of the ^1H chemical shifts in wild-type eglin and the double mutant for the regions in the vicinity of the mutation site. These are the residues Ser41–Tyr49 in the binding loop and the strand Asn50–Phe55 whose side chains interact with the binding loop via hydrogen bonds. Residues that are not listed in Table II have identical chemical shifts in both proteins. All backbone resonances are identical except for residues Val43–Arg48, and both Arg51 and Arg53 which interact with the binding loop. The most significant difference is an upfield shift of the backbone amide proton of the mutated residue Ser46 in position P1′ of the double mutant compared to Asp46 in the wild-type protein. As has been mentioned above, the side chain of Asp46 in wild-type eglin forms a hydrogen bond to its own amide proton, according to the crystal structure of eglin c in complex with subtilisin Carlsberg (Bode et al., 1986a, 1987; McPhalen & James, 1988). The pH titration experiments described below provide evidence that this hydrogen bond also exists in the free protein in solution.

The $N^\epsilon H$ of Arg51 has an unusually large downfield shift (9.12 ppm) in both wild-type eglin and mutant L45R/D46S compared to approximately 6.6 ppm in random coil peptides (Bundi & Wüthrich, 1979). This indicates that this atom is forming a strong hydrogen bond, which is the C-terminal carboxyl group of Gly70 as found in the crystal structure of eglin. It also shows that the interaction of the side chain of Arg51 with Gly70 is unperturbed in the double mutant L45R/D46S. For comparison, the $N^\epsilon H$ resonances of Arg22, Arg48, and Arg53 are at 7.01, 7.30, and 7.32 ppm, respectively, indicating that these $N^\epsilon H$ groups are not involved in intramolecular hydrogen bonds. The $N^\eta H$ resonances of Arg51 have been assigned from NOESY spectra. They show two broad intraresidue cross-peaks to the $N^\epsilon H$ resonance. Their position is almost the same in the double mutant (Table III). There is little known in the literature about the influence of hydrogen bonding on arginine $N^\eta H$ resonances, and there are not many cases where these resonances have been assigned in proteins. In the crystal structures of the proteinase complexes the $N^\eta H$ protons are involved in hydrogen bonds with the Asp46 side chain. In the double mutant, one of these resonances is shifted to higher field by 0.14 ppm. This may indicate a weakening or loss of this hydrogen bond.

pH Titration Experiments. The pH dependence of the amide proton resonances of wild-type eglin c was studied with 2D heteronuclear ^{15}N–^1H correlated experiments. Spectra at 14 pH values from 1.85 to 5.72 were recorded. The pK_a values and the titration shifts, $\Delta\delta$, of resonances of the binding loop region are listed in Table IV. There are only two carboxylates in this region of the protein, Asp46 and the C-terminus. The peptide NH of Asp46 titrates with a pK_a of 2.8 by the amount of –0.28 ppm. This indicates that the side chain of Asp46 has a pK_a of 2.8 and forms a hydrogen

Table III: Comparison of the Proton Chemical Shifts[a] of Mutant L45R/D46S and Wild-Type (in Parentheses) Eglin (at pH 3.0, 36 °C)

residue	NH	H^{α}	$H^{\beta 2}$, $H^{\beta 3}$	$H^{\gamma 1}$, $H^{\gamma 2}$	others
Ser41	7.72 (7.72)	4.61 (4.61)	3.86, 3.96, (3.86, 3.96)		
Pro42		4.48 (4.49)	1.88, 2.28 (1.88, 2.25)	2.02, 2.10 (2.02, 2.10)	(3.92, 3.72)
Val43	8.12 (8.07)	4.53 (4.57)	2.11 (2.11)	0.84, 0.95 (0.84, 0.95)	
Thr4	7.76 (7.66)	4.43 (4.36)	4.38 (4.30)	1.23 (1.21)	
Arg45	8.62 (8.60)	4.31 (4.46)			
Ser46	7.68 (8.16)	4.32 (4.45)	3.82, 3.91 (2.65, 2.74)		
Leu47	8.34 (8.13)	4.70 (4.72)	1.45, 1.53 (1.38, 1.45)	(1.30)	H^{δ}: 0.83, 0.90 (0.80, 0.86)
Arg48	8.90 (8.82)	4.53 (4.56)	1.56, 1.83 (1.56, 1.82)	1.53 (1.53)	H^{δ}: 3.15 (3.15)
					$N^{\epsilon}H$: 7.28 (7.30)
Tyr49	8.47 (8.46)	4.28 (4.28)	2.85, 3.31 (2.85, 3.31)		H^{δ}: 7.15 (7.15)
					H^{ϵ}: 6.83 (6.83)
Asn50	7.94 (7.94)	4.96 (4.96)	2.63, 3.25 (2.63, 3.25)		H^{δ}: 7.63, 7.84 (7.63, 6.89)
Arg51	7.30 (7.29)	5.40 (5.37)	1.45, 2.29 (1.45, 2.29)	1.79 (1.79)	H^{δ}: 2.85, 2.93 (2.85, 2.93)
					$N^{\epsilon}H$: 9.16 (9.12)
					$N^{\eta}H$: 6.44, 6.64 (6.58, 6.64)
Val52	8.37 (8.37)	4.13 (4.13)	1.20 (1.20)	0.19, 0.19 (0.19, 0.19)	
Arg53	8.67 (8.62)	4.43 (4.43)	1.49, 1.76 (1.49, 1.76)	0.89, 1.19 (0.89, 1.21)	H^{δ}: (2.90, 3.14)
					$N^{\epsilon}H$: (7.32)
Val54	8.69 (8.70)	4.13 (4.13)	1.41 (1.41)	0.18, 0.98 (0.18, 0.98)	
Phe55	9.21 (9.21)	6.08 (6.08)	2.72, 2.83 (2.72, 2.83)		H^{δ}: 7.13 (7.13)
					H^{ϵ}: 7.05 (7.05)
					H^{ζ}: 7.13 (7.13)
Val69	8.53 (8.53)	4.65 (4.67)	2.15 (2.15)	1.18, 1.09 (1.18, 1.09)	
Gly70	8.83 (8.84)	3.42, 4.34 (3.42, 4.34)			

[a] Only resonances of residues close to the mutation site are listed. Stereospecific assignments were obtained for those β-methylene protons and for those γ-methyl protons of valines that are underlined (Hyberts et al., 1987).

Table IV: NH Resonances of the Vicinity of the Binding Loop with Significant pH Titration shifts[a]

residue	number	pK_a	$\Delta\delta$
Thr	44	<2.0; ~2.8	+0.32
Leu	45	<2.0	−0.19
Asp	46	2.8	−0.28
Leu	47	~2.8	+0.14
Arg	48	<2.0	−0.20
$ArgH^{\epsilon}$	51	<2.0	−1.42

[a] The titration shift $\Delta\delta$ is the total chemical shift change between pH 1.85 and 5.72. Negative values are for shifts to lower field with increasing pH, indicating hydrogen bonds to titrable groups.

bond to its own amide proton. From the difference between this pK_a and the pK_a of aspartic acid in random coil peptides, which is 3.9 (Bundi & Wüthrich, 1979), we estimate the strength of the hydrogen bond as $\Delta\Delta G = 0.68$ kcal/mol (using the formula $\Delta\Delta G = RT\,\Delta pK_a$). The $N^{\epsilon}H$ resonance of Arg51 has a constant chemical shift of 9.12 ppm between pH 2.5 and 6. It shifts strongly to higher field with the pH decreasing below pH 2.5. At the lowest pH (1.85) where we recorded a spectrum, the pH dependence is steepest, indicating that the pK_a of the interacting titrable group is lower than 2.0. The titrable group causing this effect can only be the C-terminal carboxy group of Gly70. This proves that the hydrogen bond between the C-terminus and the $N^{\epsilon}H$ of Arg51, seen in the crystal structure of the complex with proteinases, is conserved in the solution structure of the free inhibitor. From the difference between the pK_a value of a free C-terminal carboxy group of ca. 3.3, we estimate the strength of this hydrogen bond as > 0.8 kcal/mol. This estimate includes, however, also all other hydrogen bonds in which this C-terminal carboxy group is involved. One of these can be identified from the pH titration experiments as the peptide NH of Arg48. It shows an upfield shift with decreasing pH with the same pK_a as the $N^{\epsilon}H$ of Arg51. The amount of the shift is significantly smaller than that of Arg51. This indicates that the hydrogen bond from the C-terminus to the Arg51 side chain is stronger than to the backbone NH of Arg48. The peptide NH groups of the residues Asp46 and Leu47 do not shift with the titration of the C-terminal Gly70 while Thr44 experiences the titration of both carboxy groups. The interpretation of the titration behavior of Thr44 is not straightforward. It shifts in the direction opposite that of the residues involved in hydrogen bonds. This apparently means that the deshielding of this amide proton becomes less efficient due to minor conformational changes when the carboxy groups get negatively charged with increasing pH and adapt stronger hydrogen bonds with their most favorable partners, other than Thr44. Generally, the residues of the binding loop, listed in Table IV, are more pH dependent than the rest of the protein.

Comparison of Temperature Coefficients in Wild-Type Eglin and Mutant L45R/D46S. The temperature coefficients of the H^N resonances for the wild-type protein and the double mutant were measured, and heteronuclear ^1H–^{15}N correlated spectra were recorded at 6, 16, 26, and 36 °C for the wild type. For the double mutant protein, spectra were recorded at 10, 20, 25, 30, and 36 °C. Figure 7 shows a comparison of these temperature coefficients for wild-type eglin and the double mutant. The first nine residues that are unstructured and solvent accessible (Hyberts & Wagner, 1989; Hyberts et al., 1992) have uniform temperature coefficients of approximately 7 ± 1 parts per billion (ppb) per degree. The values for the rest of the molecule show a large variation; therefore, an obvious classification of amides in two groups with small and large temperature coefficients, respectively, is not possible. In this context, however, we found that all temperature coefficients, in particular those of the binding loop including residue 46, are identical in the wild-type and the double mutant, within the errors of measurements. This is a strong indication that the hydrogen bond patterns involving main chain amide protons are very similar in wild-type eglin c and the double mutant. For residue 46, it seems that the peptide NH is involved in similar hydrogen bonds in the wild type and in the double mutant, but the hydrogen bond is weaker in the mutant L45R/D46S. Thus, the loss of the inhibitory activity seems mainly to be a consequence of differences in protein dynamics.

Comparison of NOEs in Wild Type and Mutant L45R/D46S. NOESY spectra of wild-type eglin and mutant L45R/D46S are nearly identical. A detailed quantitative analysis of the NOEs in wild-type protein has been carried out, and

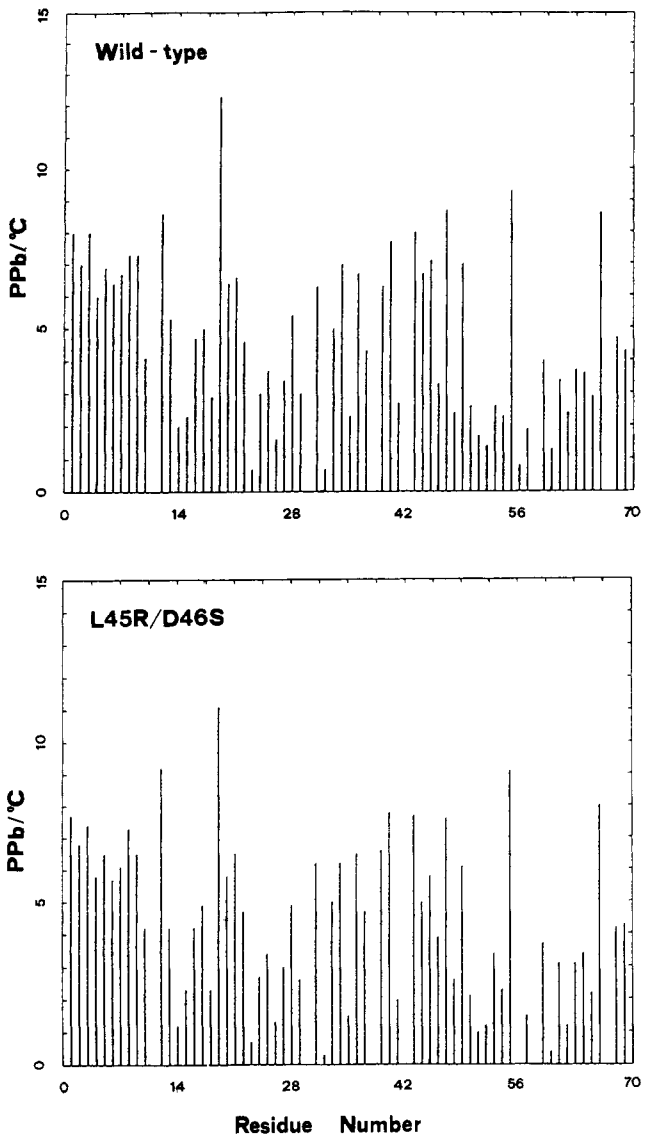

FIGURE 7: Comparison of the temperature coefficients of the amide proton resonances in eglin: (a) wild type and (b) L45R/D46S mutant. The temperature coefficients were measured from ^{15}N–^{1}H correlated spectra.

a high-precision structure has been determined (Hyberts et al., 1992). NOESY spectra at long mixing times (200 ms) were completely assigned, and NOESY cross-peak volumes in spectra with 50-ms mixing times were quantitatively measured. A similar quantitative analysis is in progress for the double mutant. At the present stage, no striking differences in the NOESY spectra could be detected.

Comparison of Coupling in Wild Type and Mutant L45R/D46S. A complete analysis of the χ^1 dihedral angles was performed by measuring the heteronuclear vicinal ^{15}N–H^{β} coupling constants and estimating the homonuclear H^{α}–H^{β} coupling constants. All χ^1 dihedral angles that could be characterized were found to be identical in the wild type and the double mutant, in particular for residues in the binding loop. Residue Asp46 in the wild-type protein and Ser46 in the double mutant have both χ^1 angles of around +60°, which is close to the value seen for Asp46 in the crystal structure of wild-type eglin. Two residues of the proteinase binding loop of free eglin c appear to have different χ^1 angles than those in the crystal structure of eglin c in the complex with subtilisin Carlsberg, both in the wild-type protein and the double mutant. These are Val43 (+60° in solution, –60° in the complex) and Leu47 (180° in solution, –60° in the crystal structure of the complex). For Val43, the coupling constants indicate that there is mobility with respect to χ^1, and +60° is only the dominant torsion angle. For Leu47 the identification of the angle is only tentative. The measurement of the homonuclear and the heteronuclear coupling constants is difficult due to the near degeneracy of the H^{β} resonances.

Comparison of ^{15}N Relaxation Parameters in Wild Type and Mutant L45R/D46S. Figure 8 shows a plot of the cross-peak intensities vs sequence in a 2D steady-state ^{15}N NOE experiment for wild-type elgin and double mutant. The values of the bars represent the intensity of the cross-peaks in the 2D heteronuclear ^{1}H–^{15}N correlated spectra after long saturation of the proton resonances. The steady-state NOE is 1 minus the intensity given in the Figure 8. Spectra were recorded as a time series with increasing irradiation times, and the data given are the results of fitting this time dependence. This gave more precise results than measuring a single spectrum with a long irradiation time. In particular, the heteronuclear NOEs are so different in eglin that steady state may be reached for one residue (for example in the rigid core) but not for another (N-terminus). Without presaturation, the intensity is 1.0, with long proton presaturation, this value goes down to 0.6–0.8, for the rigid parts of the protein. More mobile parts of the protein have values significantly below this level (Figure 8). In wild-type eglin c, most nitrogens have intensities in the heteronuclear NOE experiment of around 0.7 with the exception of the mobile N-terminal residues Thr1–Lys8 that have values as low as –2.4 Also, the residues Thr44, Leu45, Asp46, and Leu47 have smaller values between 0.4 and 0.6, indicating that the binding loop is significantly more mobile than the core of the protein. In the double mutant L45R/D46S, the cross-peak intensity in the heteronuclear NOE for residue Ser46 is around –0.1. This demonstrates that the mutation D46S dramatically increases the mobility of the scissile bond. Similar observations are made in measurements of the longitudinal relaxation times T_1 and the transverse relaxation times T_2, or $T_{1\rho}$, respectively. The latter value changes by 30% of the double mutant. The assignments of the H–N cross-peak of Asp46 and Ser46 in wild-type and mutant protein, respectively, have been checked carefully in 2D NOESY, and 3D ^{15}N dispersed TOCSY spectra. A detailed account of ^{15}N relaxation measurements in eglin c and the double mutant will be presented elsewhere.

DISCUSSION

Change in the Inhibitory Specificity of Eglin. In many serine proteinase inhibitor families, a large variety of amino acids are found in position P1, a phenomenon called the "hypervariability" of the reactive site (Laskowski & Kato, 1980) which finds its zenith in the third domains of avian ovomucoids where eight alternative amino acids were found in position P1 (Laskowski et al., 1981, 1987). Therefore, serine proteinase inhibitors can be regarded as an exception to the rule that functionally important residues are strongly conserved in evolution. To a first approximation, the specificity of serine proteinase inhibitors is mainly determined by the shape and the character of the S1 pocket of the respective target enzyme, i.e., the high preference of trypsin for basic amino acids is due to its extended S1 pocket with a negatively charged residue at its bottom (Huber et al., 1974). These findings suggest that it might be well possible to change the inhibitory specificity of serine proteinase inhibitors by exchanging amino acids in position P1.

This approach was very successful for the L45R eglin mutant where a clear-cut specificity change of eglin was engineered.

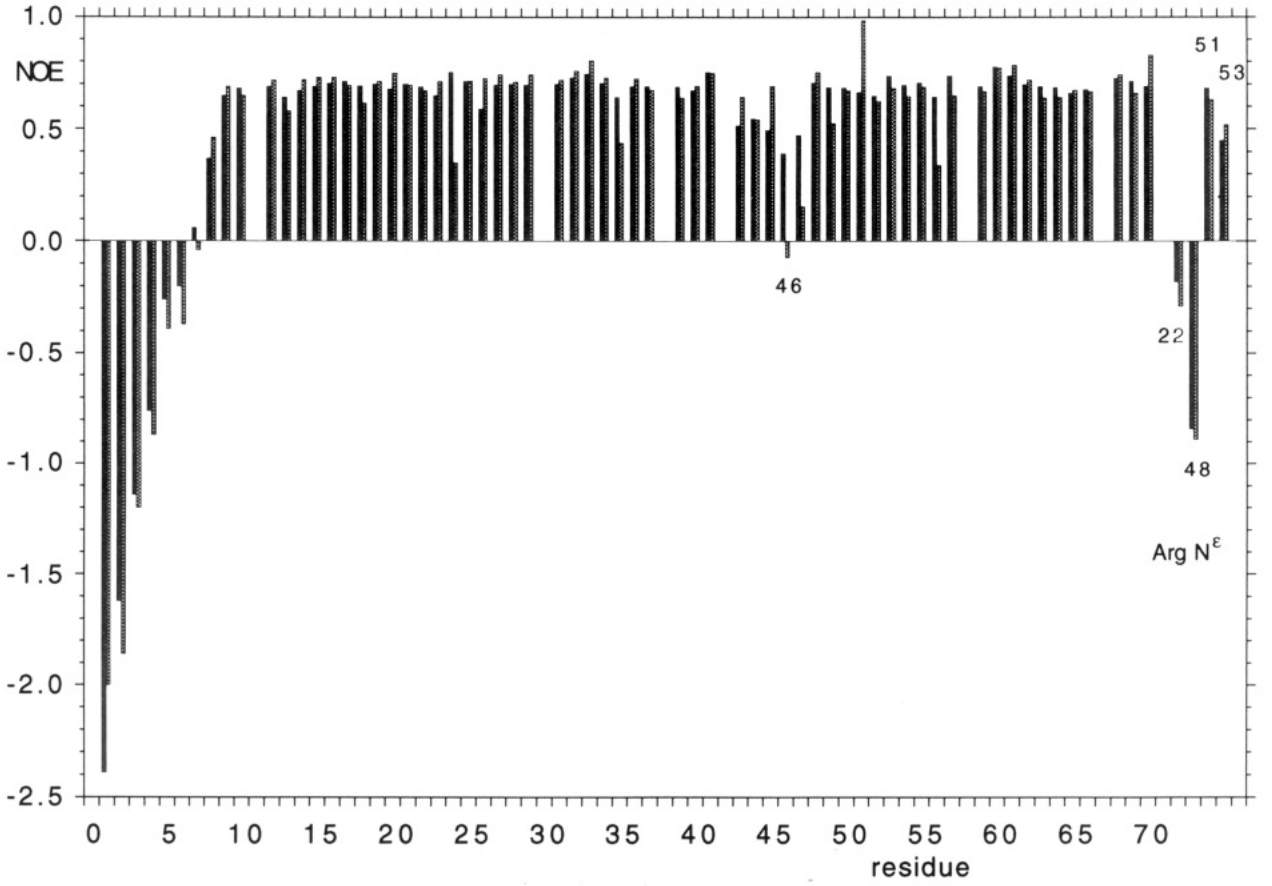

FIGURE 8: Plot of the heteronuclear steady-state NOEs of ^{15}N nuclei in eglin vs the amino acid sequence. Solid and dashed bars are for the wild type and the L45R/D46S mutant, respectively. The value of the columns represents the intensity of the ^{15}N resonance of the residue while saturating the ^{1}H resonances. The details of the experiment are described by Peng and Wagner (1992). The last four columns represent the parameters for the N^{ϵ} resonances of the four arginines in positions 22, 48, 51, and 53. The latter two have side chains involved in intramolecular hydrogen bonds.

L45R eglin is a potent trypsin inhibitor with a K_i of 2.5×10^{-11} M, a value which lies well in the range of natural trypsin inhibitors. L45R eglin is a weak HLE inhibitor which parallels the weak inhibition of trypsin by wild-type eglin. This clearly shows that a residue in position P1 in eglin determines largely its inhibitory specificity. The result complements similar experiments performed on a variety of different proteinase inhibitors: The chemical mutation of Arg63 → Trp in soybean trypsin inhibitor changed its specificity toward α-chymotrypsin (Leary & Laskowski, 1973). Semisynthetic methods have been used to replace Lys15 (P1) in BPTI with arginine, valine, phenylalanine, and tryptophan (Jering & Tschesche, 1976). The specificity of BPTI could be changed from trypsin to elastase inhibition by the mutation Lys15 → Val (Wenzel et al., 1986), which represents a reversal of our results described in this paper. The natural mutation of Met358 → Arg in α1-proteinase inhibitor changed the elastase inhibitor to a thrombin inhibitor (Pittsburgh mutant), resulting in a fatal bleeding disorder in a patient (Owen et al., 1983). These results were confirmed by in vitro mutagenesis (Jallat et al., 1986). McWerter et al. (1989) systematically studied mutants in position P1 of the *Curcurbita maxima* trypsin inhibitor and created novel inhibitors for HLE and cathepsin G. The inhibitory specificity of chymotrypsin inhibitor 2, an inhibitor highly homologous to eglin, was changed from chymotrypsin to trypsin ($K_i = 5.6 \times 10^{-9}$ M) by mutating Met59 (P1) to lysine (Longstaff et al., 1990). The replacement of Leu18 (P1) with glutamate converted the third domain of the turkey ovomucoid into a powerful inhibitor of Glu-specific *Streptomyces griseus* proteinase (Komiyama et al., 1991). The Kunitz-type inhibitor domain of Alzheimer's β-amyloid precursor protein was changed from a trypsin to an HLE inhibitor by changing the putative P1 arginine to a valine (Sinha et al., 1991). The model structure of the complex between mutant L45R and trypsin shows an excellent fit of Arg45 into the S1 binding pocket of trypsin which is the first necessary requirement for a desired specificity change. The superposition of mutant L45R on BPTI shows the second necessary requirement, a good agreement in the contribution of the binding loops, which are complementary to the respective target enzyme. A specificity change caused by point mutations in position P1 is only possible if the whole binding loop of the inhibitor is highly complementary to the active site of the target enzyme, too.

Mutant L45R is still a strong subtilisin inhibitor which reflects the promiscuity of the large active site pocket of subtilisin. BPTI, however, does not inhibit subtilisin, despite a very similar binding loop conformation compared to the strong subtilisin inhibitor eglin. The reason is the presence of a bulky secondary binding loop, which interferes with binding to subtilisin (Hirono et al., 1979). This example shows that even the presence of a highly complementary binding loop together with the "correct" P1 amino acid in proteinase inhibitors is often not sufficient for the inhibition of a new target enzyme.

Mutants L45R and especially L45R/D46S do not inhibit thrombin which can be explained by the extended binding loop of eglin which unfavorably interferes with the narrow active site cleft of thrombin (Bode et al., 1989b), which probably prevents efficient binding. This result suggests that

the binding loop structure of mutant L45R/D46S differs significantly from those in natural thrombin inhibitors, despite having a "conserved" arginine and serine in positions P1 and P1′, respectively. In summary, we suggest the exchange of amino acids in position P1 of serine proteinase inhibitors as a general means to change their specificity, as long as the reactive site loop of the inhibitor is highly complementary to the active site of the target proteinase and provided no unfavorable interferences occur between both molecules.

Binding Loop Stabilization in Eglin. On the basis of sequence comparisons, mutant T44P (position P2) was designed to increase its binding to HLE. Instead, it showed a 10-fold higher K_i for HLE. Thr44 in wild-type eglin interacts via two hydrogen bonds with the side chain of Arg53 in the core of the molecule. One of these hydrogen bonds (i.e., between atom O1 of Thr44 and Arg53) is lost in mutant T44P. Despite the possibly improved binding of mutant T44P to elastase due to a proline residue in position P2, the loss of this important hydrogen bond leads to a weakening of the binding loop stabilization which causes a decrease in the inhibitory activity. A complementary situation is found in mutant R53K. The crystal structure of this mutant, which is a 100-fold weaker inhibitor of HLE, similarly shows the loss of both important hydrogen bonds formed between residues 44 and 53 in wild-type eglin. The missing hydrogen bonding potential is partially restored by a tightly bound solvent molecule which is situated exactly between both residues in mutant R53K (Heinz et al., 1991).

The noncovalent interactions between residues 44 and 53 parallel the role of disulfide bridges formed between cysteines in positions P2 (or P3) and the core of the inhibitor as found in many other serine proteinase inhibitors (Laskowski & Kato, 1980). The selective reduction of the disulfide bridge between Cys14 (P2) and Cys38 in BPTI converted the inhibitor of trypsin to a substrate (Jering & Tschesche, 1976), demonstrating the importance of these interactions for binding loop stabilization.

Both mutants T44P and R53K are HLE inhibitors, T44P, however, became a substrate of subtilisin in contrast to R53K. This behavior can be understood by considering the structure differences of the active sites between HLE (Bode et al., 1986b) and subtilisin. The S2 pocket of HLE (lined by the flat side of His57, Leu99, and Phe215) is very hydrophobic and can well accommodate a proline in position P2 (Figure 6). The additional binding energy provided by these favorable interactions probably compensates for the lack of one hydrogen bond important for the binding loop stabilization. The S2 pocket in subtilisin is less hydrophobic (Thr33, His64, Leu96, and a solvent molecule) than in HLE, which might lead to weaker interactions with mutant T44P and a subsequent cleavage of the weaker inhibitor and an easier release of the cleaved product.

Mutant R51K became a weaker HLE inhibitor and a substrate of subtilisin. In the absence of experimental structural data on this mutant, the only explanation of its weaker inhibitory potential is the loss of interactions between Asp46 and Arg51 (hypothetical model in Figure 5) which most likely increases the mobility of the binding loop. The investigation of this mutant by NMR spectroscopy is underway (Dayie & Wagner, unpublished results). The ^{1}H NMR spectrum has been assigned, and the secondary structures have been characterized. They are clearly the same as in the wild-type protein. However, the resonance positions of many residues, in particular in the binding loop, are largely changed. The mutant also has generally weaker NOE's and seems to be more "floppy" than the wild-type protein or the L45R/D46S double mutant. It can be expected that in the tertiary structure of this mutant the position of the binding loop relative to the core of the protein is significantly different from the wild-type and the double mutant. It appears that the R51K mutation destabilizes the interaction of the core of the protein with binding loop while the internal rigidity of the binding loop is conserved, so that some proteinase inhibitory activity is maintained. This is an effect just opposite to that in the double mutant L45R/D46S.

Mutant L45R/D46S was found to be a substrate of the serine proteinases trypsin, HLE, and subtilisin. The mutant was thoroughly investigated by 2D-NMR spectroscopy. The composition of the ^{1}H chemical shifts of wild-type eglin and mutant L45R/D46S revealed as the major difference an upfield shift of the backbone amide proton of residue 46 of 0.48 ppm. In random coil peptides, serine and aspartic acid have identical chemical shifts for the amide proton and the α-proton (Bundi & Wüthrich, 1979). Therefore, the different covalent structure cannot be made responsible for this chemical shift change. Also, there are no aromatic side chains near this residue. Therefore, changed ring current shifts cannot cause the change of the resonance position of the amide proton of residue 46. It has been recognized before that amide proton resonances are very sensitive to hydrogen bonding, and a clear relationship between hydrogen bond length and downfield shift has been found (Wagner et al., 1983; Pardi et al., 1983). Thus, the observed upfield shift of the amide proton of Ser46 in mutant L45R/D46S led to the hypothesis that the mutation Asp46 → Ser results in the loss or weakening of the intraresidue hydrogen bond between the backbone amide proton and its own side chain (Wagner et al., 1990), which interaction is suggested by the crystal structure of eglin (Bode et al., 1986a). The pH titration experiments (Table IV) indicate that such a hydrogen bond exists also in the free inhibitor and is not just a consequence of the formation of the complex with the proteinase.

A commonly used method for studying hydrogen bonding in polypeptides and proteins in solution is the measurement of the temperature dependence of the amide proton chemical shifts. It has been shown, for example, in small cyclic peptides (Schwyzer et al., 1972) that resonances of amide protons that are involved in intramolecular hydrogen bonds exhibit a small temperature coefficient close to zero while resonances of amide protons that are exposed to the solvent have a significantly larger temperature coefficient of about 0.006 ppm/deg. This phenomenological distinction seems to hold to some degree for proteins. Recently, we have measured the temperature coefficients of the amide resonances for the basic pancreatic trypsin inhibitor for which a refined high-resolution crystal structure is available (Huber et al., 1974). We find that resonances of amide protons involved in intramolecular hydrogen bonds always show smaller temperature coefficients than amide protons exposed to solvent (Clubb and Wagner, unpublished results). All amide protons of BPTI that are involved in intramolecular hydrogen bonds have temperature coefficients of less than 0.005 ppm/deg. However, the distinction between amide protons involved in intramolecular versus intermolecular hydrogen bonds with water is not that clear as it seems to be in small molecules. Therefore, this spectroscopic aspect may not be valuable to identify intramolecular hydrogen bonds as such, but it may give qualitative information about changes in hydrogen bonding patterns between related molecules.

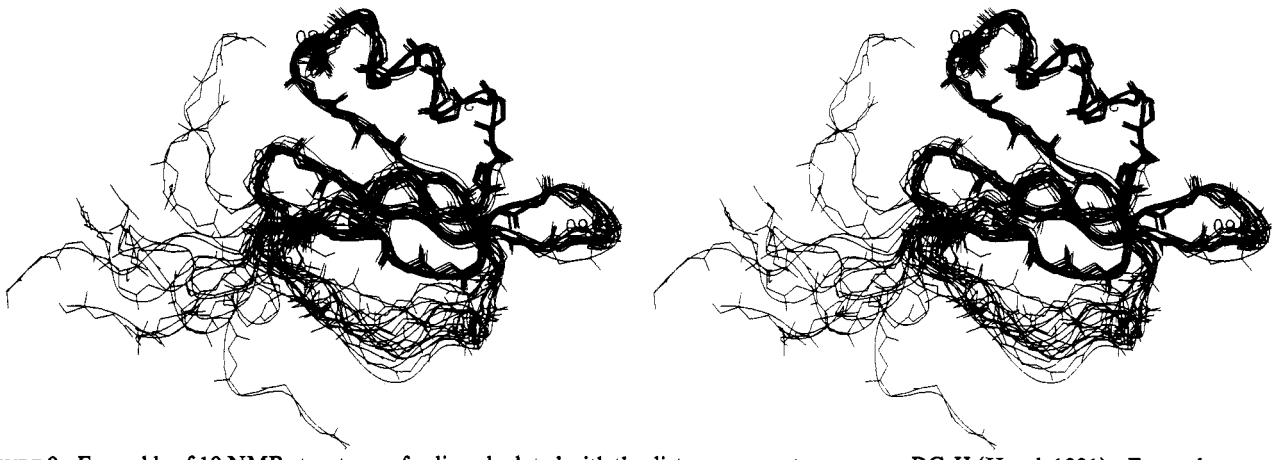

FIGURE 9: Ensemble of 10 NMR structures of eglin calculated with the distance geometry program DG-II (Havel, 1991). For each structure, a spline is given to represent the peptide fold.

In mutant L45R/D46S, we find no significant difference in the temperature coefficients when compared to those in wild-type eglin (Figure 7). The value is slightly higher than for the wild-type protein but by far not as high as for the residues of the mobile N-terminus. This indicates that the amide group of Ser46 is also involved in intramolecular, but probably weaker, hydrogen bonds.

Mobility of the N–H bond vectors can readily be studied with measurements of ^{15}N relaxation parameters, such as the longitudinal and transverse relaxation times T_1 and T_2, respectively, the ^1H–^{15}N heteronuclear nuclear Overhauser effect (NOE), and ^1H–^{15}N heteronuclear cross-relaxation rates σ_{HN}. For molecules of the size of eglin and a field strength of 11.745 T (500-MHz proton frequency), internal mobility is most significantly manifested in the heteronuclear NOEs. For large molecules without internal mobility, the heteronuclear ^1H–^{15}N NOE is expected to be 0.82 (this value is different from 1 since relaxation by chemical shift anisotropy plays a role (Peng & Wagner, 1992)). For internal motion the heteronuclear NOE is expected to be a negative number which reaches its theoretical limit at –3.6. In wild-type and double mutant eglin c, the heteronuclear NOEs are very similar (Figure 8). The only significant difference in the ^1H–^{15}N NOE relaxation parameters in mutant L45R/D46S compared to wild-type eglin is a much smaller heteronuclear NOE for residue Ser46 compared to Asp46 (Figure 8). This shows that the mutation Asp46 → Ser dramatically increases the mobility of the N–H bond vector of residue 46. On the other hand, the mobility of the side chains of R53 and R51 is essentially unchanged as monitored by the relaxation parameters of the $^{15}N^{\epsilon}$ (Figure 8). Thus, we conclude that the interaction of the core with the binding loop is essentially conserved but the internal mobility of the binding loop is increased.

Figure 9 shows a set of calculated NMR structures of wild-type eglin. Details of the structure determination are described elsewhere (Hyberts et al., 1992). In this context, we focus on the conformation of the binding loop. While the backbone of the core of the protein has average root mean square differences (rmsd) to the mean coordinates of approximately 0.4 Å, the average rmsd for the binding loop is as large as 2.0 Å. Analysis of the backbone dihedral angles shows that the peptide bonds 38–39 and 46–47 seem to act as hinges causing this motion, as also observed by Heinz et al. (1991), while residues 43–45 have a relatively rigid backbone structure. The flapping mobility may be necessary to provide the necessary adaptability of the inhibitor to fit into the proteinase active site. The relative rigidity of the loop in itself is required to prevent cleavage of the inhibitor. The D46S mutation alone destroys the relative rigidity of the peptide bond 45–46, as observed by the relaxation time experiments so that the local rigidity required for function as an inhibitor is lost.

The reasons for the loss of local rigidity are not obvious, as there is little definite understanding of what makes a molecule rigid or flexible. The strength of the interaction between the side chains of residues 46 and 51 may certainly decrease with the exchange of an asparagine with a serine; the fact that the link of these two side chains is shorter in the double mutant may distort the local structure so that the structure of the bound water molecules nearby is changed. The double mutant is significantly less stable against denaturation by heat than the wild type protein, indicating that some favorable interaction is lost.

In summary, we conclude that already very subtle changes of the extensive hydrogen bonding pattern formed between the binding loop and the core in eglin can determine the fate of the molecule as being an inhibitor or a substrate of serine proteinases. Although the conformations of wild-type and mutant eglin are virtually identical, the loss of inhibitory activity is manifested in the dynamic properties of the protein. There seem to be three aspects that affect the inhibitory activity of the mutants: (i) The surface of the inhibitor is changed so that the fit with the complementary surface of the proteinase is perturbed. This aspect was probed with mutants T44P and L45R. (ii) The internal stability of the binding loop is perturbed. This has been probed with the L45R/D46S mutant which leaves the overall structure completely conserved but reduces the rigidity of the backbone around the scissile bond leading to a loss of the inhibitory function. (iii) The interaction of the binding loop with the core of the protein is perturbed. This has been probed with the R51K mutant which has a changed conformation while the binding loop appears to maintain its rigidity. This seems to be sufficient to maintain some inhibitory activity.

ACKNOWLEDGMENT

The help of W. Raschdorf, Drs. H.-P. Schnebli, N. J. Braun, P. Moser, and F. Barth is kindly acknowledged as well as the excellent technical assistance of J. Rahuel and M. Carvajal. We thank the referees for helpful comments.

REFERENCES

Anil Kumar, Ernst, R. R., & Wüthrich, K. (1980) *Biochem. Biophys. Res. Commun. 95*, 1–6.

Barber, M., Bordoli, R. S., Elliott, G. J., Tyler, A. N., Bill, J. C., & Green, B. N. (1984) *Biomed. Mass Spectrom. 11*, 182–186.
Bieth, J. (1974) in *Proteinase Inhibitors, Bayer Symposium 5* (Fritz, H., Tschesche, H., Greene, L. J., & Truscheit, E. eds.) Springer, Berlin, pp. 463–469.
Bode, W., & Huber, R. (1992) *Eur. J. Biochem. 204*, 433–451.
Bode, W., Papamokos, E., Musil, D., Seemueller, U., & Fritz, H. (1986a) *EMBO J. 5*, 813–818.
Bode, W., Wei, A.-Z., Huber, R., Meyer, E., Travis, J., & Neumann, S. (1986b) *EMBO J. 5*, 2453–2458.
Bode, W., Papamokos, E., & Musil, D. (1987) *Eur. J. Biochem. 166*, 673–692.
Bode, W., Meyer, E., & Powers, J. C. (1989a) *Biochemistry 28*, 1951–1963.
Bode, W., Mayr, I., Baumann, U., Huber, R., Stone, S. R., & Hofsteenge, J. (1989b) *EMBO J. 8*, 3467–3475.
Braun, N. J., Bodmer, J. L., Virca, G. D., Metz-Virca, G., Maschler, R., Bieth, J. G., & Schnebli, H.-P. (1987) *Biol. Chem. Hoppe-Seyler 368*, 299–308.
Braunschweiler, L., & Ernst, R. R. (1983) *J. Magn. Reson. 53*, 521–528.
Bundi, A., & Wüthrich, K. (1979) *Biopolymers 18*, 285–298.
Chase, T., Jr., & Shaw, E. (1970) *Methods Enzymol. 14*, 20–27.
Clarke, L., & Carbon, J. (1978) *J. Mol. Biol. 120*, 517–532.
Grunstein, M., & Hogness, D. S. (1975) *Proc. Natl. Acad. Sci. U.S.A. 72*, 3961–3965.
Havel, T. F. (1991) *Prog. Biophys. Mol. Biol. 56*, 43–78.
Heinz, D. W. (1990) Ph.D. Thesis, University of Basel, Switzerland.
Heinz, D. W., Priestle, J. P., Rahuel, J., Wilson, K. S., & Grütter, M. G. (1991) *J. Mol. Biol. 217*, 353–371.
Hirono, S., Nakamura, K. T., Iitaka, Y., & Mitsui, Y. (1979) *J. Mol. Biol. 131*, 855–869.
Hörl, H., & Heidland, A., Eds. (1982) *Adv. Exp. Med. Biol. 167*.
Huber, R., Kukla, D., Bode, W., Schwager, P., Bartels, K., Deisenhofer, J., & Steigemann, W. (1974) *J. Mol. Biol. 89*, 73–101.
Hyberts, S. G., Märki, W., & Wagner, G. (1987) *Eur. J. Biochem. 164*, 625–635.
Hyberts, S. G., & Wagner, G. (1989) *Biochemistry 29*, 1465–1474.
Hyberts, S. G., Goldberg, M., Havel, T. F., & Wagner, G. (1992) *Protein Sci.* (in press).
Jallat, S., Carvallo, D., Tessier, L. H., Roeklin, D., Roitsch, C., Ogushi, F., Crystal, R. G., & Courtney, M. (1986) *Protein Eng. 1*, 29–35.
Jeener, J., Meier, B. H., Bachmann, P., & Ernst, R. R. (1979) *J. Chem. Phys. 71*, 4546.
Jering, H., & Tschesche, H. (1976) *Eur. J. Biochem. 61*, 443–463.
Jones, T. A. (1978) *J. Appl. Crystallogr. 11*, 268–272.
Kramer, B., Kramer, W., & Fritz, H.-J. (1984) *Cell 38*, 879–887.
Kojima, S., Nishiyama, Y., Kumagai, I., & Miura, K. (1991) *J. Biochem. 109*, 377–382.
Komiyama, T., Bigler, T. L., Yoshida, N., Kosaku, N., & Laskowski, M., Jr. (1991) *J. Biol. Chem. 266*, 10727–10730.
Laemmli, U. K. (1970) *Nature 227*, 680–685.
Laskowski, M., & Kato, I. (1980) *Annu. Rev. Biochem. 49*, 593–626.
Laskowski, M., Empie, M. W., Kato, I., Kohr, W. J., Ardelt, W., Bogard, W. C., Weber, E., Papamokos, E., Bode, W., & Huber, R. (1981) in *32. Colloquium der Gesellschaft für Biologsiche Chemie* (Eggerer, H., & Huber, R., Eds.) pp 136–152, Springer, Berlin.
Laskowski, M., Kato, I., Ardelt, W., Cook, J., Denton, A., Empie, M. W., Kohr, W. J., Park, S. J., Parks, K., Schatzley, B. L., Schoenberger, O. L., Tashiro, M., Vichot, G., Whatley, H. E., Wieczorek, A., & Wieczorek, M. (1987) *Biochemistry 26*, 202–221.
Leary, T. R., & Laskowski, M. (1973) *Fed. Proc. 32*, 465.
Longstaff, C., Campbell, A. F., & Fersht, A. R. (1990) *Biochemistry 29*, 7339–7347.
Macura, S., Huang, Y., Suter, D., & Ernst, R. R. (1981) *J. Magn. Reson. 43*, 259–281.
McPhalen, C. A., Schnebli, H. P., & James, M. N. G. (1985) *FEBS Lett. 188*, 55–58.
McPhalen, C. A., & James, M. N. G. (1988) *Biochemistry 27*, 6582–6598.
McWherter, C. A., Walkenhorst, W. F., Campbell, E. J., & Glover, G. I. (1989) *Biochemistry 28*, 5708–5714.
Messing, J. (1983) *Methods Enzymol. 101*, 20–78.
Michal, G. (1984) *Methods Enzym. Anal. 1*, 86–104.
Montelione, G. T., Winkler, M. E., Rauenbuehler, P., & Wagner, G. (1989) *J. Magn. Reson. 82*, 198–204.
Neurath, H. (1984) *Science 224*, 350–357.
Owen, M. C., Brennon, S. O., Lewis, J. H., & Carrell, R. W. (1983) *N. Engl. J. Med. 309*, 694–698.
Pardi, A., Wagner, G., & Wüthrich, K. (1983) *Eur. J. Biochem. 137*, 445–454.
Peng, J. W., & Wagner, G. (1992) *J. Magn. Reson.* (in press).
Peng, J. W., Thanabal, V., & Wagner, G. (1991) *J. Magn. Reson. 94*, 82–100.
Pflugrath, J. W., Saper, M. A., & Quiocho, F. A. (1984) in *The Methods and Applications in Crystallographic Computing* (Hall, S., & Ashida, T., Eds.) p 404, Oxford University Press, Oxford.
Priestle, J. P. (1988) *J. Appl. Crystallogr. 21*, 572–578.
Read, R. J., & James, M. N. G. (1986) in *Proteinase Inhibitors* (Barrett, A. J., & Salvesen, G., Eds.) pp 193–208, Elsevier, Amsterdam.
Rink, H., Liersch, M., Sieber, P., & Meyer, F. (1984) *Nucleic Acids Res. 12*, 6369–6387.
Sanger, F., Nicklen, S., & Coulson, A. R. (1977) *Proc. Natl. Acad. Sci. U.S.A. 74*, 5463–5467.
Schechter, I., & Berger, A. (1967) *Biochem. Biophys. Res. Commun. 27*, 157–162.
Schnebli, H. P., & Braun, N. J. (1986) in *Proteinase Inhibitors* (Barrett, A. J., & Salvesen, G., Eds.) pp 613–627, Elsevier, Amsterdam.
Schwyzer, R., Grathwohl, C., Meraldi, J. P., Tun-Kyi, A., Vogel, R., & Wüthrich, K. (1972) *Helv. Chim. Acta 55*, 2545.
Seemüller, U., Meier, M., Ohlsson, K., Müller, H.-P., & Fritz, H. (1977) *Hoppe–Seyler's Z. Physiol. Chem. 358*, 1105–1117.
Seemüller, U., Eulitz, M., Fritz, H., & Strobl, A. (1980) *Hoppe-Seyler's Z. Physiol. Chem. 361*, 1841–1846.
Shaka, A. J., Lee, C. J., & Pines, A. (1988) *J. Magn. Reson. 77*, 274–293.
Sinha, S., Knops, J., Esch, F., Moyer, E. D., & Oltersdorf, T. (1991) *J. Biol. Chem. 31*, 21011–21013.
Stone, S. R., & Hofsteenge, J. (1986) *Biochemistry 25*, 4622–4628.
Vindusek, D. A., Roberts, M. F., & Bodenhausen, G. (1982) *J. Am. Chem. Soc. 104*, 5452.
Wagner, G., & Wüthrich, K. (1982) *J. Mol. Biol. 155*, 347–384.
Wagner, G., Pardi, A., & Wüthrich, K. (1983) *J. Am. Chem. Soc. 105*, 5948–5949.
Wagner, G., Hyberts, S. G., Heinz, D. W., & Grütter, M. (1990) in *Structure & Methods, Vol. 2: DNA Complexes & Proteins* (Sarma & Sarma, Eds.) pp 93–101, Adenine Press, Albany, NY.
Wenzel, H. R., Beckman, J., Mehlich, A., Schnabel, E., & Tschesche, H. (1986) in *Chemistry of Peptides and Proteins 3* (Voelter, W., Orchinnikov, Y. A., & Bayer, E., Eds.) pp 105–117, Walter de Gruyter, Berlin.
Wider, G., Neri, D., Otting, G., & Wüthrich, K. (1989) *J. Magn. Reson. 85*, 426–431.
Zoller, M. J., & Smith, M. (1983) *Methods Enzymol. 100*, 468–500.

Registry No. Eglin C, 96380-69-7; elastase, 9004-06-2; trypsin, 9002-07-7; subtilisin, 9014-01-1; serine proteinase, 37259-58-8.